Asymmetric Magnetic Reconnection in the Solar Atmosphere

Nick Murphy

Harvard-Smithsonian Center for Astrophysics

October 23, 2013

NASA Goddard Space Flight Center

Collaborators and Co-Conspirators: John Raymond, Mari Paz Miralles, Kathy Reeves, Chengcai Shen, Jun Lin, Lei Ni, Clare Parnell, Andrew Haynes, Trae Winter, Carl Sovinec, Dan Seaton, Aad van Ballegooijen, Mitsuo Oka, Aleida Young, Drake Ranquist, and Crystal Pope

Outline

- Observational signatures of asymmetric reconnection in two-ribbon flares and CMEs
- The plasmoid instability during asymmetric inflow reconnection
- What does it mean for a magnetic null point to move?

Models of CMEs often predict a reconnecting current sheet behind the rising flux rope

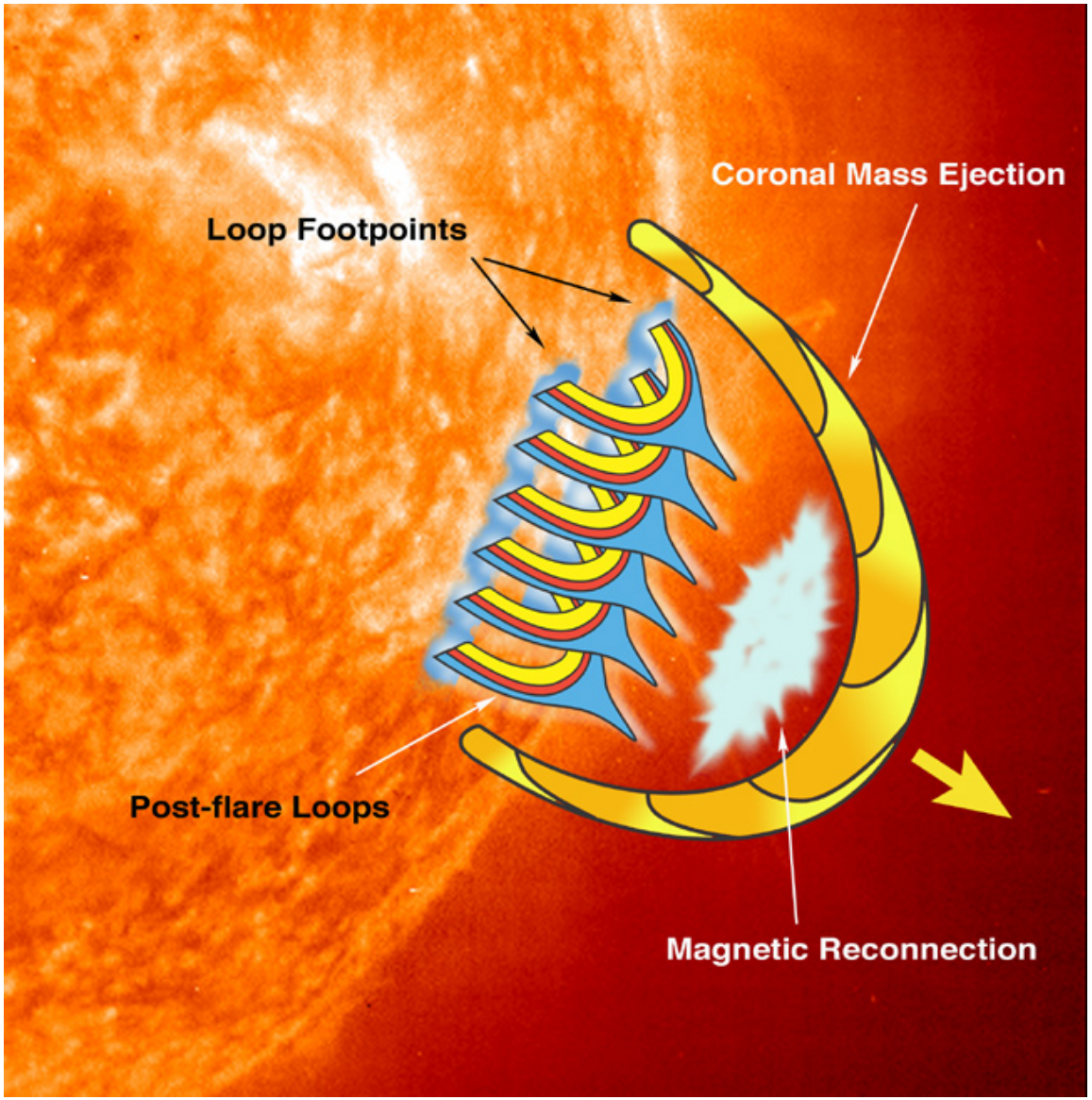

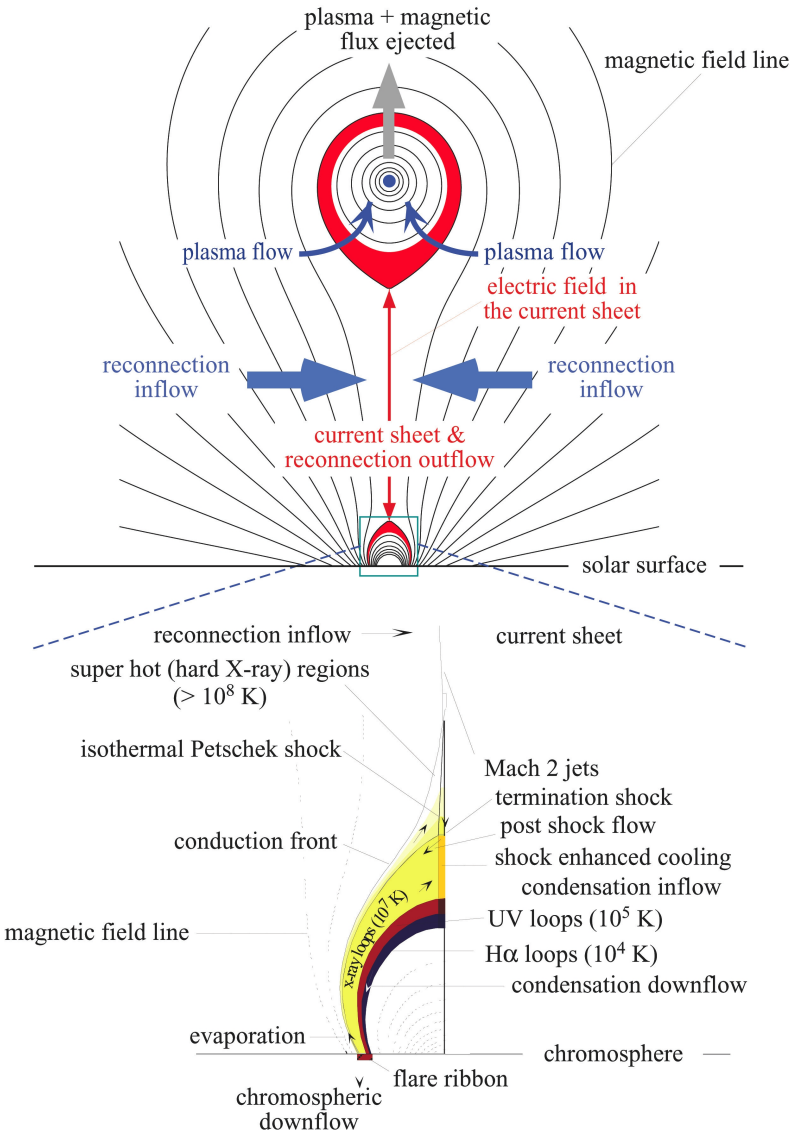

Models of CMEs often predict a reconnecting current sheet behind the rising flux rope

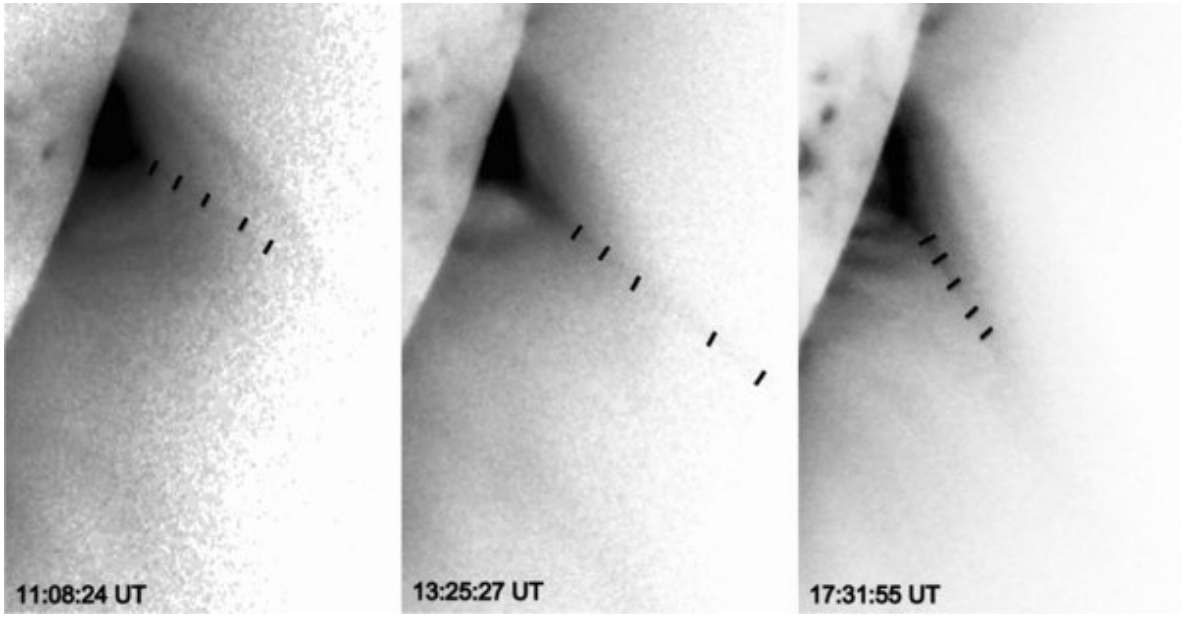

'Cartwheel CME'
Savage et al. (2010)
Hinode/XRT

- Observational signatures of this model include:
  - Ray-like structures (observed in X-rays, EUV, white light)
  - Inflows/outflows
  - Flare loop structures
  - Hard X-ray emission at loop footpoints where nonthermal particles hit chromosphere
  - Apparent motion of footpoints of newly reconnected loops
- How does asymmetry modify these observational signatures?

Asymmetric Magnetic Reconnection

- Most models of reconnection assume symmetry
- However, asymmetric magnetic reconnection occurs in the solar atmosphere, solar wind, space/astrophysical plasmas, and laboratory experiments
- *Asymmetric inflow reconnection* occurs when the upstream magnetic fields and/or plasma parameters differ
  - Solar jets: emerging flux interacting with overlying flux
  - Earth's dayside magnetopause
  - Tearing modes in tokamaks and other confined plasmas
- *Asymmetric outflow reconnection* occurs when conditions in the outflow regions are different
  - Solar flare and CME current sheets
  - Earth's magnetotail
  - Spheromak merging experiments
- There are also 3D asymmetries (e.g., patchy reconnection)

Cassak & Shay (2007) consider the scaling of asymmetric inflow reconnection

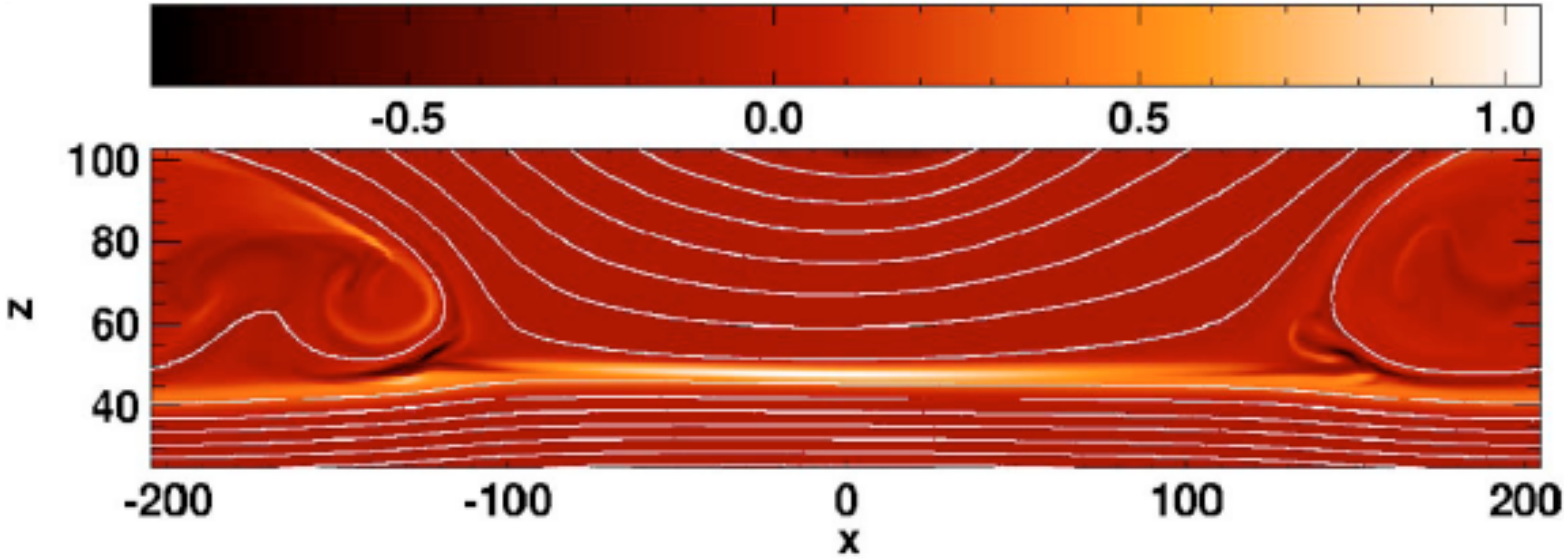

- Assume Sweet-Parker-like reconnection with different upstream magnetic fields (B_L, B_R) and densities (ρ_L, ρ_R)
- The outflow velocity scales as a hybrid Alfvén velocity:

$$V_{out} \sim V_{Ah} \equiv \sqrt{\frac{B_L B_R (B_L + B_R)}{\rho_L B_R + \rho_R B_L}} \tag{1}$$

- The X-point and flow stagnation point are not colocated

Part I: Observational Signatures of Asymmetric Reconnection in Solar Eruptions

How does magnetic asymmetry impact the standard model of two-ribbon solar flares?

- We use NIMROD to perform resistive MHD simulations of line-tied asymmetric reconnection (Murphy et al. 2012)
- Asymmetric upstream magnetic fields

$$B_y(x) = \frac{B_0}{1+b} \tanh\left(\frac{x}{\delta_0} - b\right) \tag{2}$$

  - Magnetic asymmetries of $B_L/B_R \in \{0.125, 0.25, 0.5, 1\}$
- Initial X-line near lower wall makes reconnection asymmetric
- Caveats: β larger than reality; unphysical upper wall BC (far from region of interest); no vertical stratification, 3D effects/guide field, or collisionless effects
- This setup allows us to:
  - Isolate the effects of magnetic asymmetry
  - Investigate the basic physics of asymmetric reconnection

The X-point is low so most released energy goes up

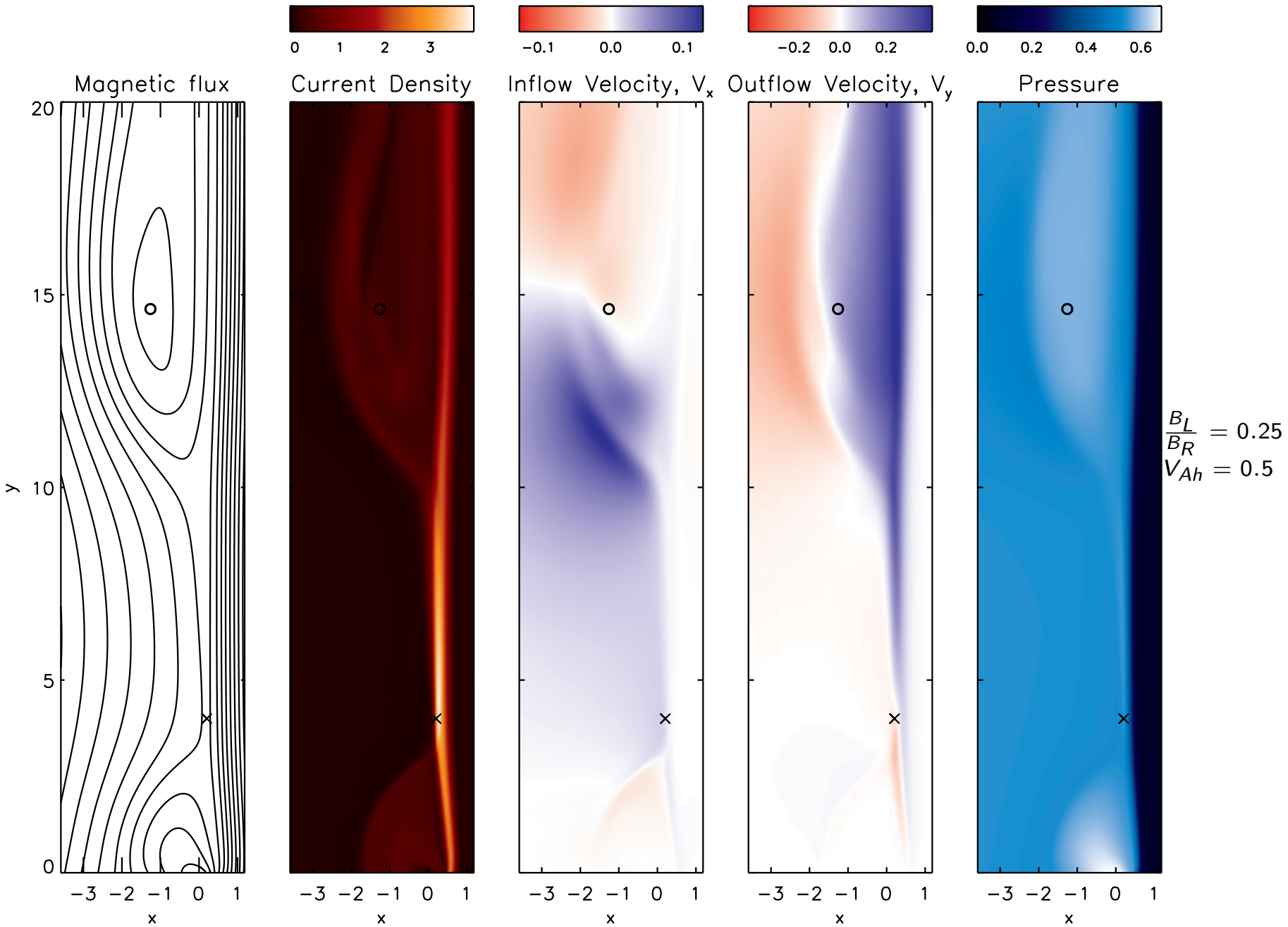

There is significant plasma flow across the X-line in both the inflow and outflow directions (see also Murphy 2010)

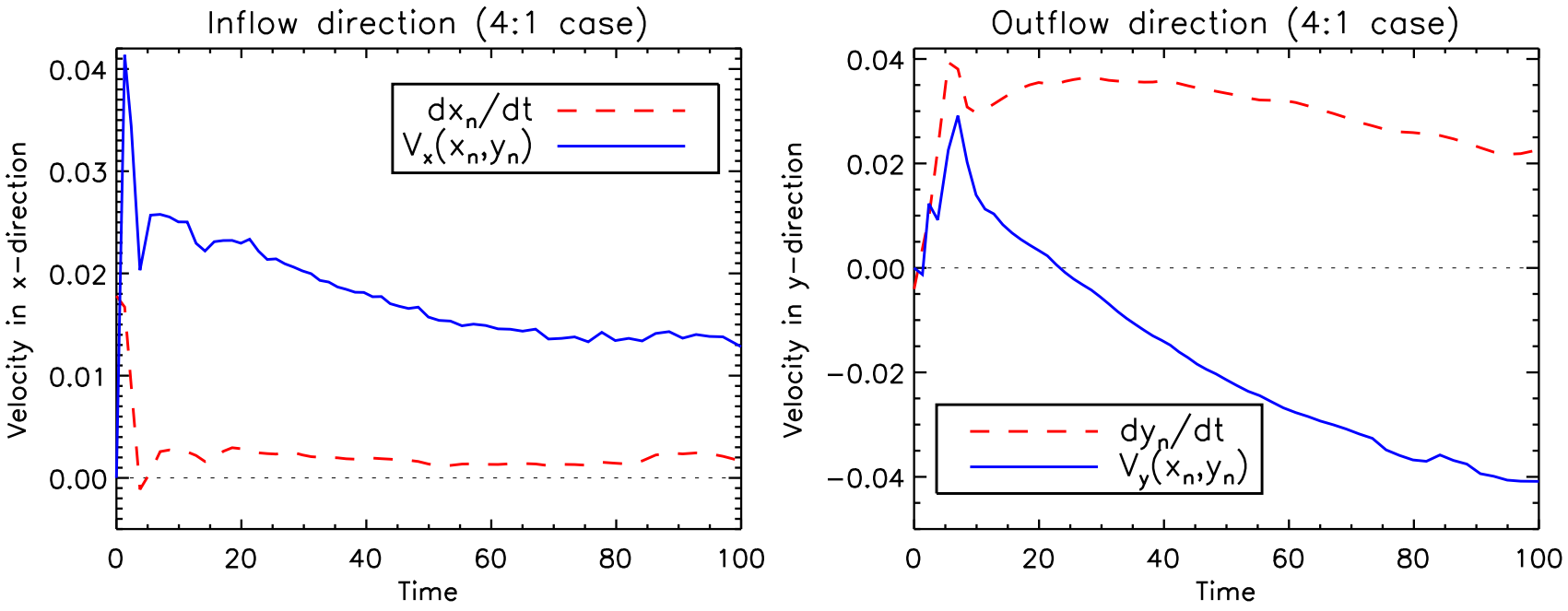

- $V_x(x_n, y_n)$ and $V_y(x_n, y_n)$ give the flow velocity at the X-line
- $\mathrm{d}x_n/\mathrm{d}t$ and $\mathrm{d}y_n/\mathrm{d}t$ give the rate of X-line motion
- For $t \gtrsim 25$, the X-line moves upward *against* the bulk flow

The flare loops develop a skewed candle flame shape

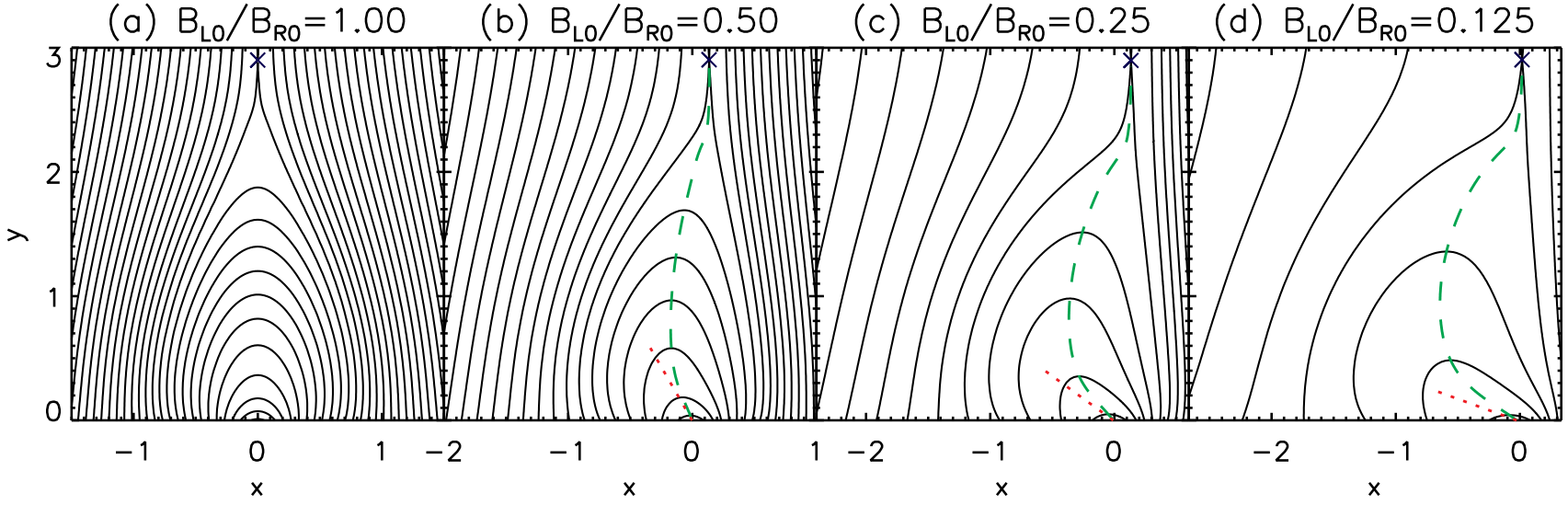

- Dashed green line: loop-top positions from simulation
- Dotted red line: analytic asymptotic approximation using potential field solution

The Tsuneta (1996) flare is a famous candidate event

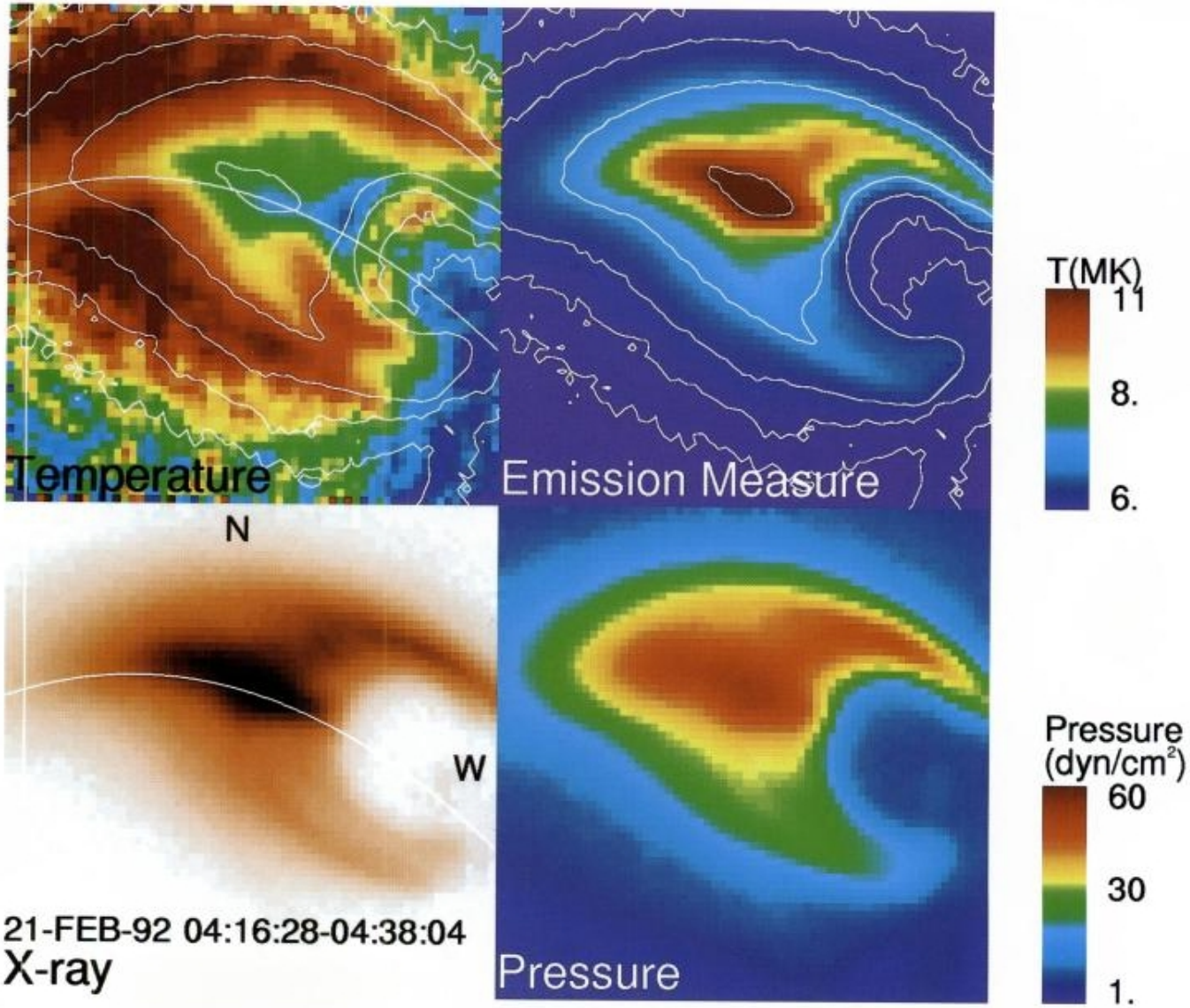

- Shape suggests north is weak **B** side

We fit simulated loops to multi-viewpoint observations to constrain the magnetic asymmetry

STEREO A

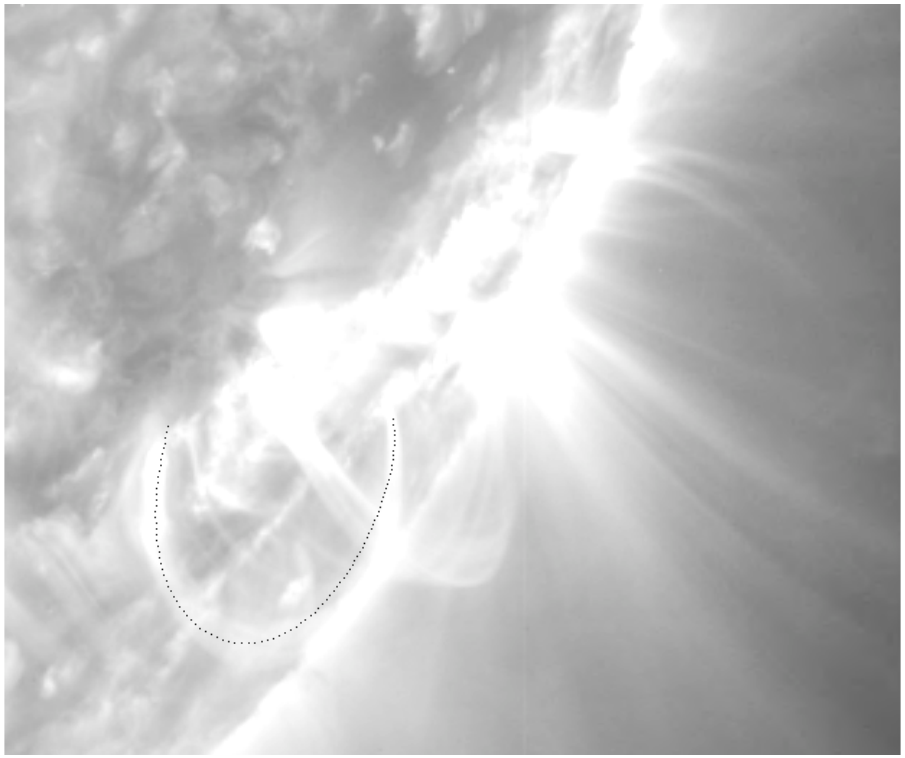

With D. Ranquist
and M. P. Miralles

- The most important constraints are
  - Location of looptop relative to footpoints
  - Different perspectives from *STEREO A/B* and *SDO*
- Results for two events: asymmetries between 1.5 and 4.0
- Symmetric simulations <u>inconsistent</u> with these observations

Asymmetric speeds of footpoint motion

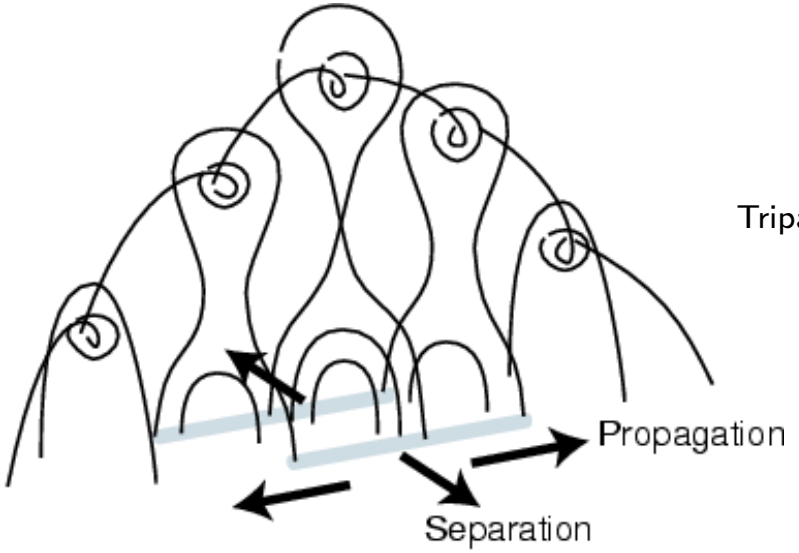

Tripathi et al. (2006)

- The footpoints of newly reconnected loops show apparent motion away from each other as more flux is reconnected
- Equal amounts of flux reconnected from each side
  $\Rightarrow$ Weak **B** footpoint moves faster than strong **B** footpoint
- Because of the patchy distribution of flux on the photosphere, more complicated motions frequently occur

Asymmetric hard X-ray (HXR) footpoint emission

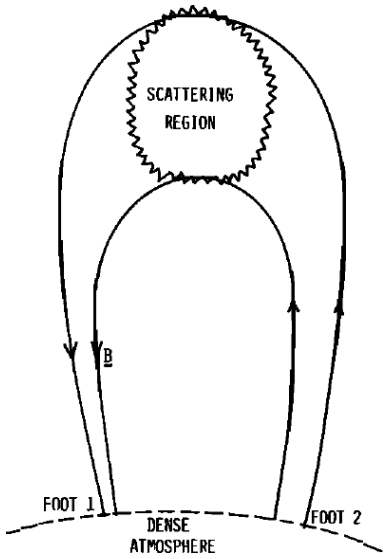

Melrose & White (1979, 1981)

- HXR emission at flare loop footpoints results from energetic particles impacting the chromosphere
- Magnetic mirroring is more effective on the strong **B** side
- More particles should escape on the weak **B** side, leading to greater HXR emission
- This trend is observed in $\sim 2/3$ of events (Goff et al. 2004)

The outflow plasmoid develops net vorticity because the reconnection jet impacts it obliquely rather than directly

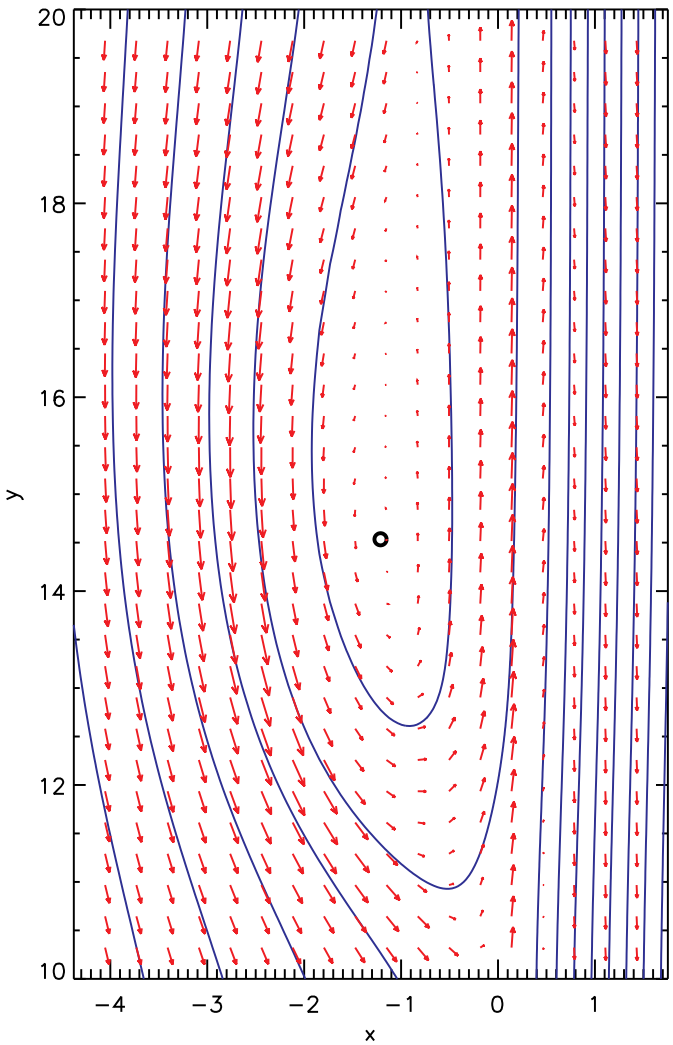

- Velocity vectors in reference frame of O-point
- Rolling motion observed in many prominence eruptions

Take away points

- Magnetic asymmetry leads to observational consequences during solar reconnection
  - Flare loops with skewed candle flame shape
  - Asymmetric footpoint motion and hard X-ray emission
  - Drifting of current sheet into strong field region
  - Rolling motions in rising flux rope
- Important effects not included in these simulations:
  - Realistic 3D magnetic geometry
  - Patchy distribution of photospheric flux
  - Vertical stratification of atmosphere
  - Collisionless effects
- Open question:
  - How can we use observation and simulation to test these predictions and determine the roles of 3D effects?

Part II: The Plasmoid Instability During Asymmetric Inflow Magnetic Reconnection

Elongated current sheets are susceptible to the plasmoid instability (Loureiro et al. 2007)

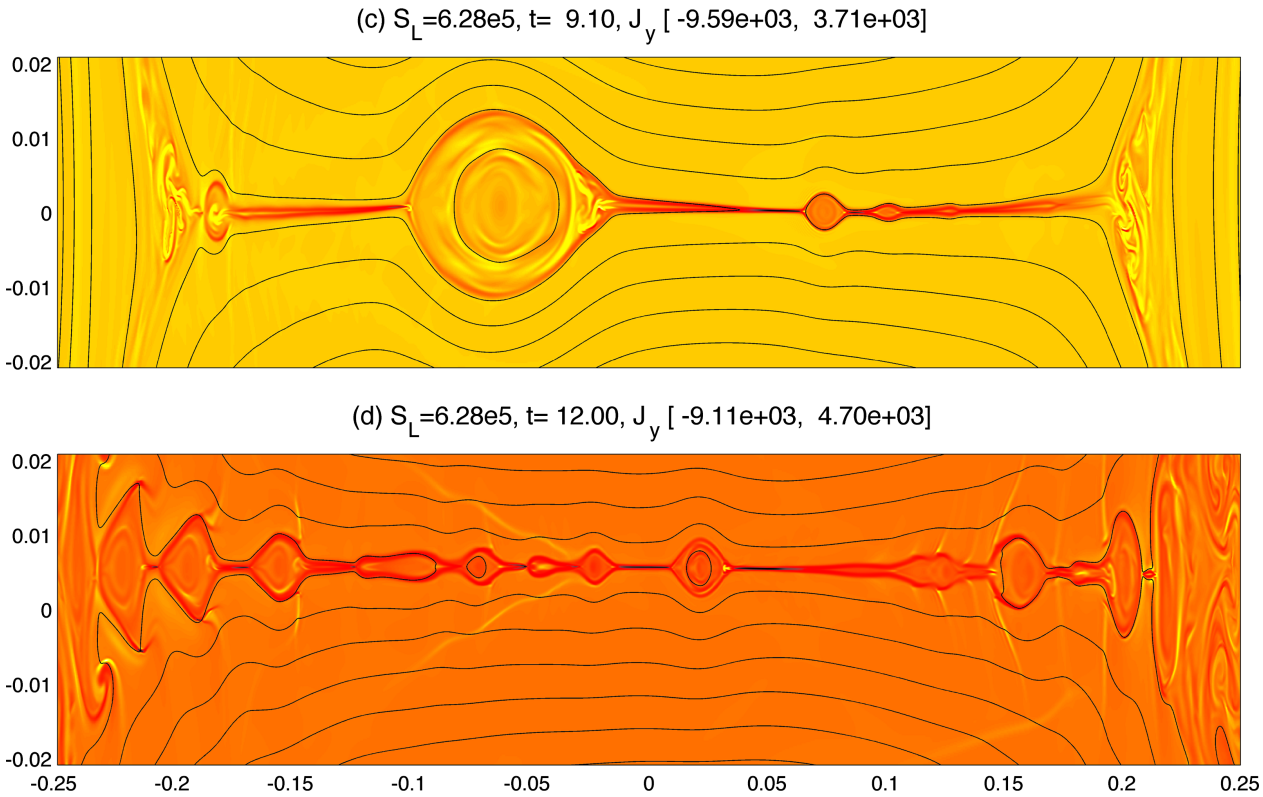

Bhattacharjee et al. (2009)
Huang et al. (2010–2013)

- The reconnection rate levels off at $\sim$0.01 for $S \gtrsim 4 \times 10^4$
- Shepherd & Cassak (2010) argue that this instability creates small enough structures for collisionless reconnection to onset
- Are CME current sheet blobs related to plasmoids? (Guo et al. 2013)

What are the dynamics of the plasmoid instability during asymmetric inflow reconnection?

- Most simulations of the plasmoid instability assume reconnection with symmetric upstream fields
  - Simplifies computing and analysis
  - Plasmoids and outflows interact in one dimension
- In 3D, flux ropes twist and writhe and sometimes bounce off each other instead of merging
  - Asymmetric simulations offer clues to 3D dynamics
- We perform NIMROD simulations of the plasmoid instability with asymmetric magnetic fields (Murphy et al. 2013)
  - (Hybrid) Lundquist numbers up to 10^5
  - Two uneven initial X-line perturbations along $z = 0$
  - $B_L/B_R \in \{0.125, 0.25, 0.5, 1\}$; $\beta_0 \geq 1$; periodic outflow BCs
  - Caveats: simple Harris sheet equilibrium; no guide field or 3D effects; resistive MHD

Plasmoid instability: symmetric inflow ($B_{L0}/B_{R0} = 1$)

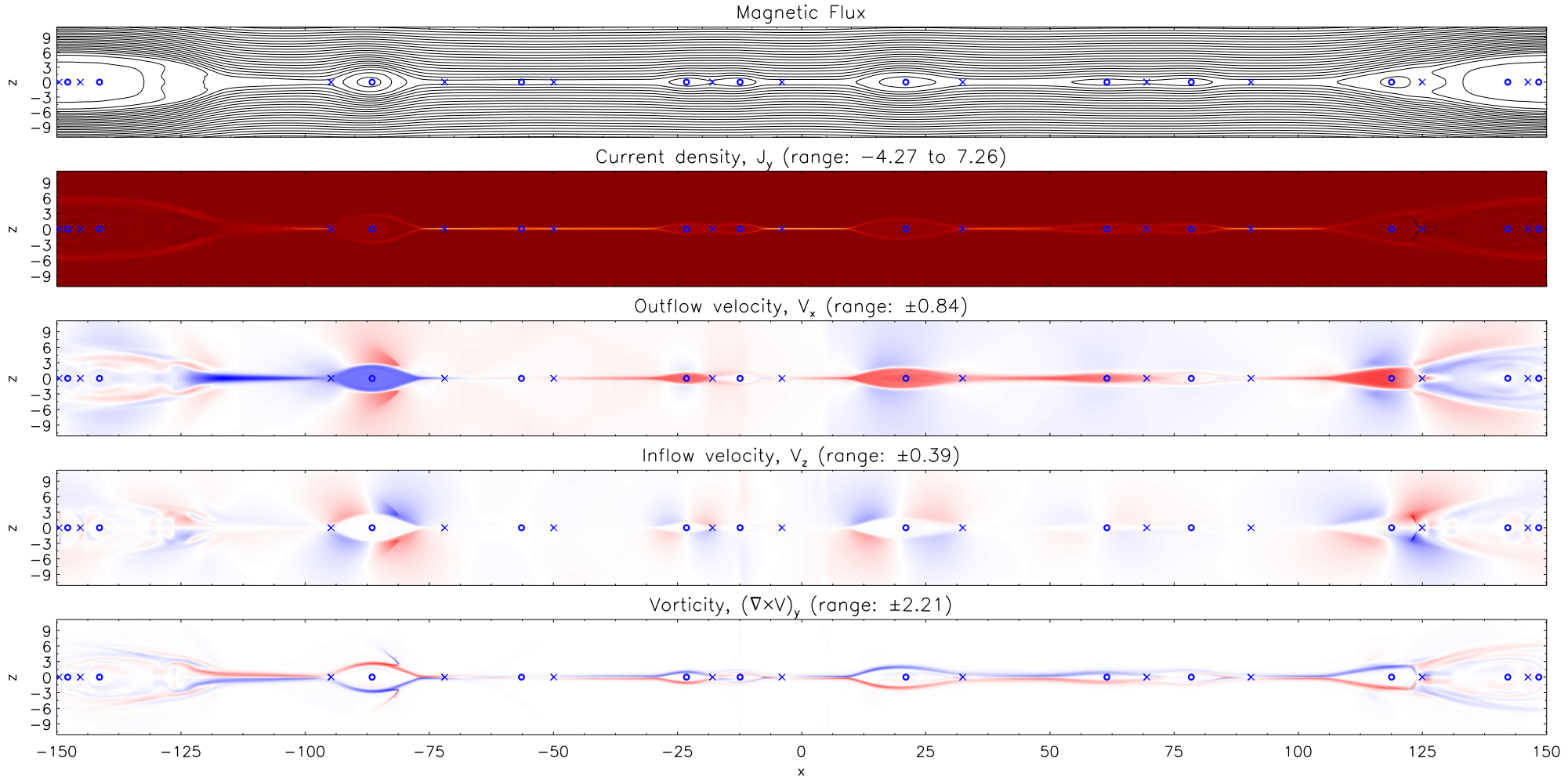

- X-points and O-points are located along symmetry axis
- X-points often located near one exit of each current sheet
- No net vorticity in islands

Plasmoid instability: asymmetric inflow ($B_{L0}/B_{R0} = 0.25$)

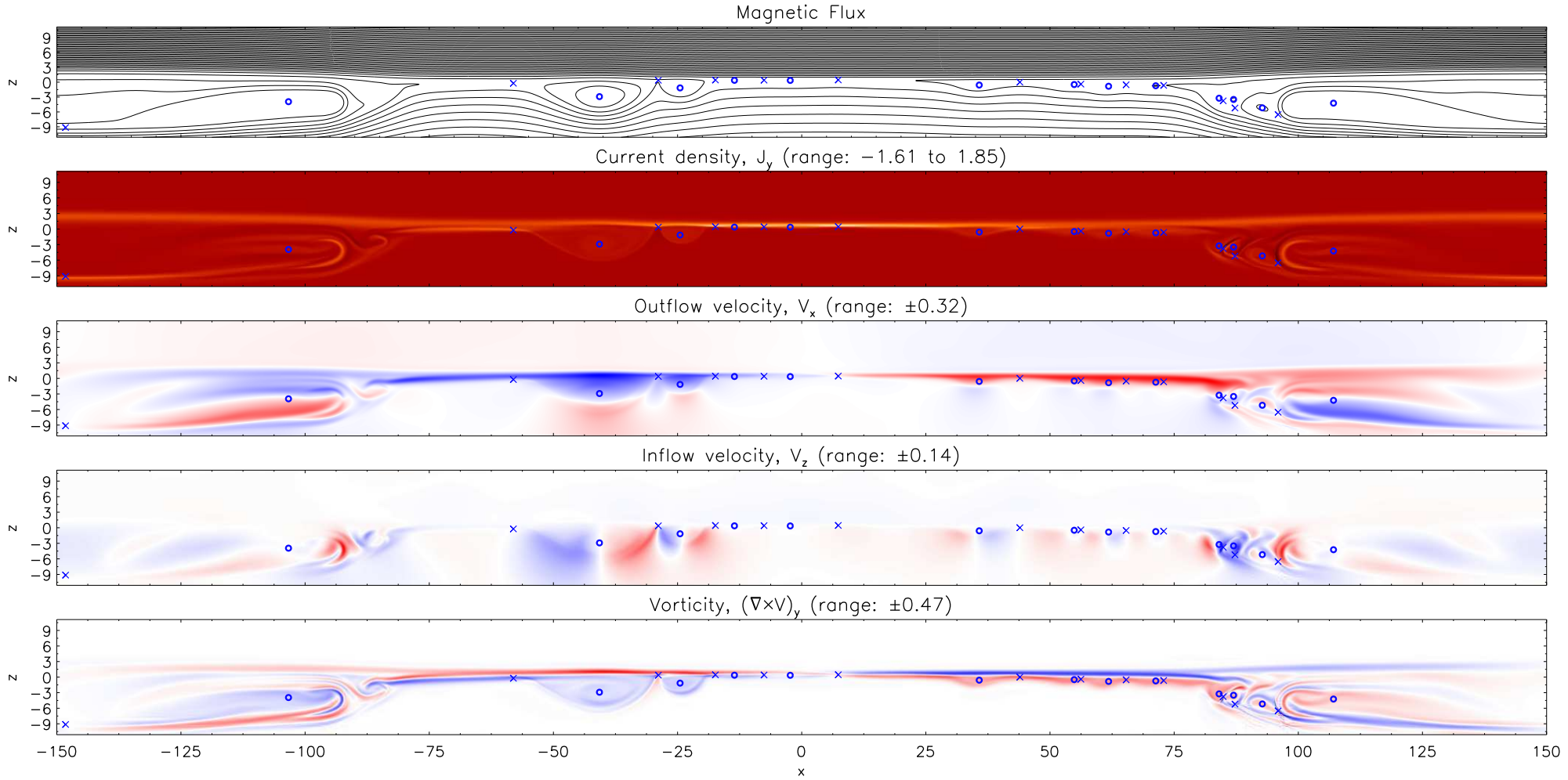

- Displacement between X-point and O-points along z direction
- Islands develop preferentially into weak field upstream region
- Islands have vorticity and downstream regions are turbulent

Secondary merging is doubly asymmetric

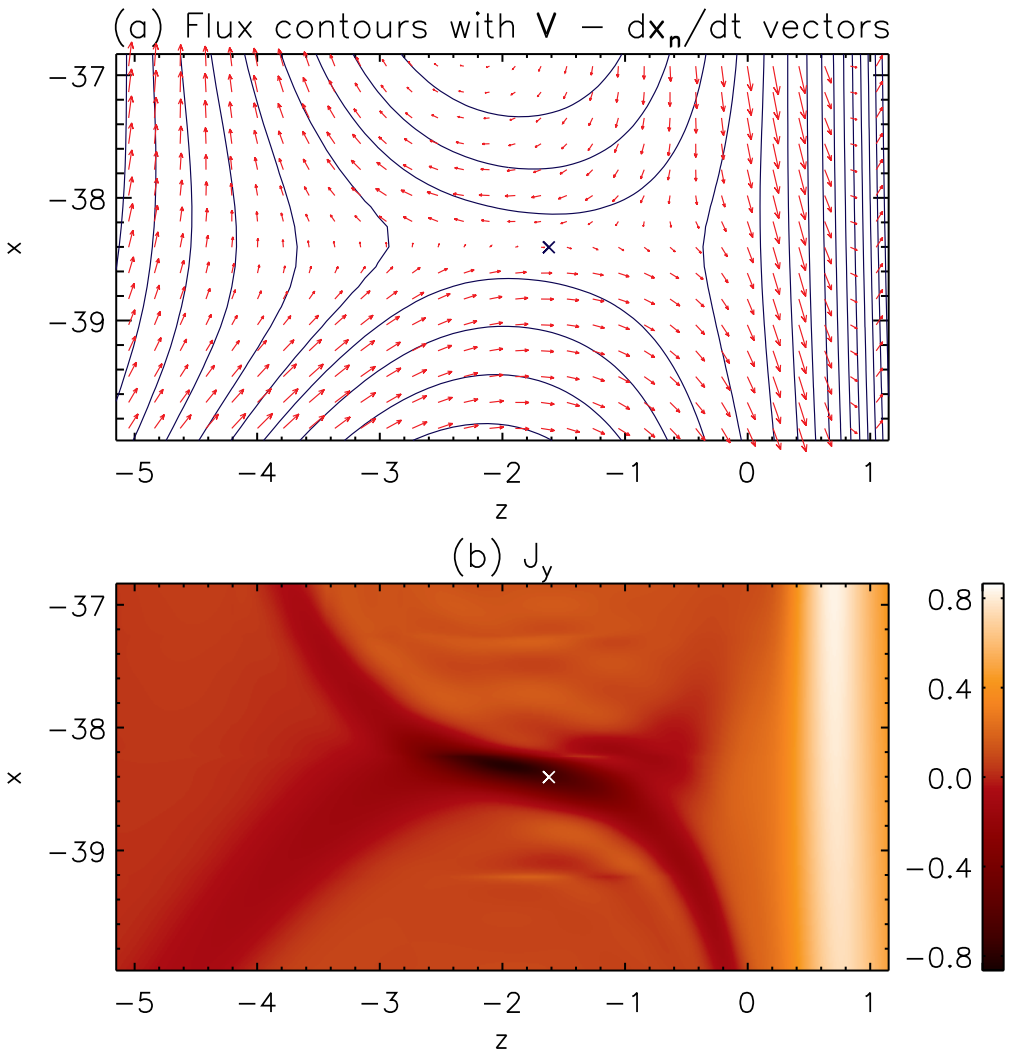

- Bottom island is much larger ⇒ island merging is not head-on
- Flow pattern dominated by shear flow associated with island vorticity ⇒ Partial stabilization of secondary reconnection

Open Questions: Asymmetric Plasmoid Instability

- What insights might these simulations provide for the 3D plasmoid instability?
  - Will merging between 'flux ropes' be less efficient?
- How do reconnection sites interact in 3D?
- What mistakes are we making by using 2D simulations to interpret fundamentally 3D behavior?

Part III: What does it mean for a magnetic null point to move?

What does it mean for a magnetic null point to move?

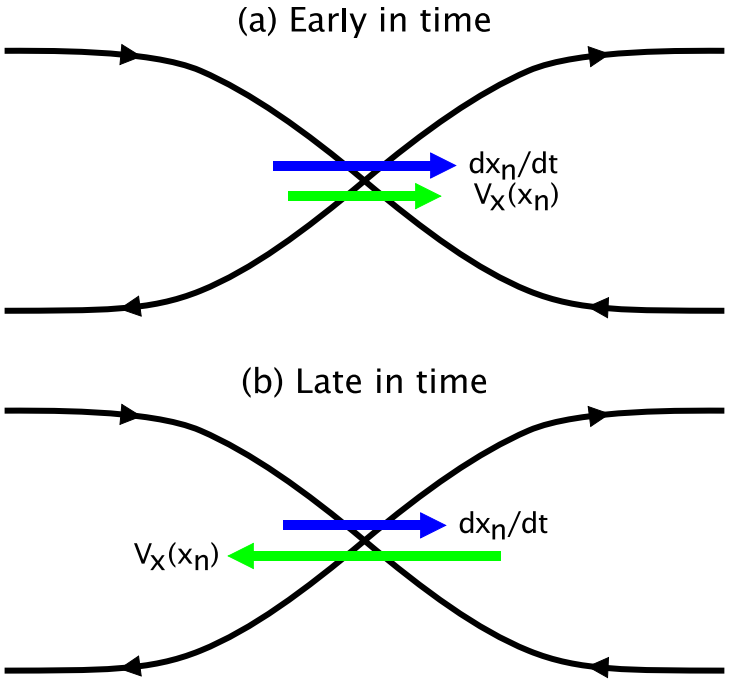

Murphy (2010)

- In these simulations, the nulls move at velocities different from the plasma flow velocity: $\frac{\mathrm{d}\mathbf{x}_n}{\mathrm{d}t} \neq \mathbf{V}(\mathbf{x}_n)$
  - Gap between flow stagnation point and magnetic field null
  - Plasma flow and X-line motion often in different directions
- To understand this, we derive an exact expression describing the motion of an isolated null point
  - We consider isolated null points because null lines and null planes are structurally unstable in 3D

Definitions

- The time-dependent position of an isolated null point is

$$\mathbf{x}_n(t) \tag{3}$$

- The null point's velocity is:

$$\mathbf{U} \equiv \frac{\mathrm{d}\mathbf{x}_n}{\mathrm{d}t} \tag{4}$$

- The Jacobian matrix of the magnetic field at the null point is

$$\mathbf{M} \equiv \begin{pmatrix} \partial_x B_x & \partial_y B_x & \partial_z B_x \\ \partial_x B_y & \partial_y B_y & \partial_z B_y \\ \partial_x B_z & \partial_y B_z & \partial_z B_z \end{pmatrix}_{\mathbf{x}_n} \tag{5}$$

The local magnetic field structure near the null is given by $\mathbf{B} = \mathbf{M}\mathbf{r}$ where $\mathbf{r}$ is the position vector.

We derive an expression for the motion of a null point in an arbitrary time-varying vector field with smooth derivatives

- First we take the derivative of the magnetic field following the motion of the magnetic field null,

$$\left.\frac{\partial \mathbf{B}}{\partial t}\right|_{\mathbf{x}_n} + \left.(\mathbf{U}\cdot\nabla)\,\mathbf{B}\right|_{\mathbf{x}_n} = 0 \tag{6}$$

  The RHS equals zero because the magnetic field will not change from zero as we follow the null point.

- Solving for $\mathbf{U}$ provides an exact expression for a null point's velocity

$$\mathbf{U} = -\mathbf{M}^{-1}\left.\frac{\partial \mathbf{B}}{\partial t}\right|_{\mathbf{x}_n} \tag{7}$$

  - Independent of Maxwell's equations
  - Unique null point velocity when $\mathbf{M}$ is non-singular

We use Faraday's law to get an expression for the motion of a null point that remains independent of Ohm's law

- Faraday's law is given exactly by

$$\frac{\partial \mathbf{B}}{\partial t} = -\nabla \times \mathbf{E} \tag{8}$$

- By applying Faraday's law to Eq. 7, we arrive at

$$\mathbf{U} = \mathbf{M}^{-1} \ \nabla \times \mathbf{E}\big|_{\mathbf{x}_n} \tag{9}$$

In resistive MHD, null point motion results from a combination of advection by the bulk plasma flow and resistive diffusion of the magnetic field

- Next, we apply the resistive MHD Ohm's law,

$$\mathbf{E} + \mathbf{V} \times \mathbf{B} = \eta \mathbf{J} \tag{10}$$

  where we assume the resistivity to be uniform.
- The expression for the rate of motion of a null point becomes

$$\mathbf{U} = \mathbf{V} - \eta \, \mathbf{M}^{-1} \, \nabla^2 \mathbf{B} \tag{11}$$

  where all quantities are evaluated at the magnetic null point. The terms on the RHS represent null point motion by
  - Bulk plasma flow
  - Resistive diffusion of the magnetic field

Murphy (2010): 1D X-line retreat via resistive diffusion

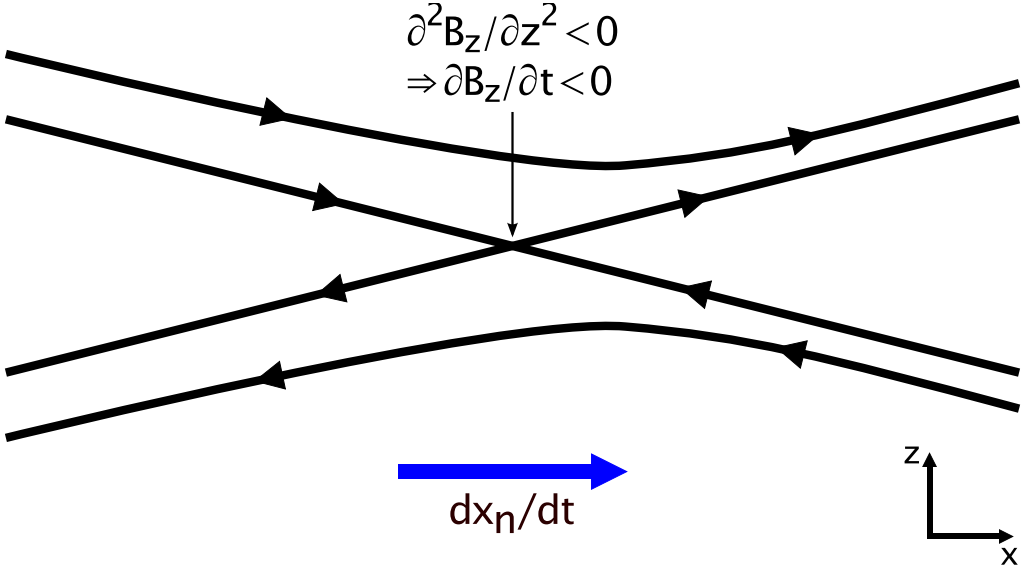

- B_z is negative above and below the X-line
- Diffusion of B_z leads to the current X-line position having negative B_z at a slightly later time
- The X-line moves to the right as a result of diffusion of the normal component of the magnetic field

$$\frac{\mathrm{d}x_n}{\mathrm{d}t} = V_x(x_n) - \eta \left[\frac{\frac{\partial^2 B_z}{\partial x^2} + \frac{\partial^2 B_z}{\partial z^2}}{\frac{\partial B_z}{\partial x}} \right]_{x_n} \tag{12}$$

What does it mean for a magnetic null point to move?

- The velocity of a null point depends intrinsically on *local* plasma parameters evaluated at the null
- Global dynamics help set the local conditions
- A unique null point velocity exists if $\mathbf{M}$ is non-singular
- Nulls are not objects and cannot be pushed by, e.g., pressure gradient forces
  - Indirect coupling between the momentum equation and the combined Faraday/Ohm's law
  - Plasma not permanently affixed to nulls in non-ideal cases
- Our expression provides a further constraint on the structures of asymmetric diffusion regions (Cassak & Shay 2007)
- How do we connect this local expression into global models?

Appearance and disappearance of null points

- In resistive MHD, nulls must diffuse in and out of existence
  - Not accounted for in bifurcation theory/topological analysis
- At instant of formation or disappearance, a null is degenerate so $\mathbf{M}$ is singular
- Nulls bifurcate in directions along which $\mathbf{B}$ and $\left.\frac{\partial \mathbf{B}}{\partial t}\right|_{\mathbf{x}_n}$ are oppositely directed
- If no such directions exist, then the degenerate null disappears
- Instantaneous velocity of separation/convergence is infinite

Conclusions

- Magnetic asymmetry during solar eruptions lead to observational consequences
  - Flare loops have a skewed candle flame shape
  - Asymmetric footpoint motion and hard X-ray emission
  - Drifting of current sheet into strong field region
  - Rolling motions in rising flux rope
- Magnetic asymmetry qualitatively changes the dynamics of the plasmoid instability
  - Islands develop into weak field upstream region
  - Jets impact islands obliquely $\Rightarrow$ net vorticity
  - Secondary merging is less efficient
- We derive an exact expression to describe the motion of magnetic null points
  - The motion of magnetic null point depends on parameters evaluated at the null
  - Null point motion in resistive MHD is caused by bulk plasma flow and diffusion of the component of $\mathbf{B}$ orthogonal to the motion